Supporting Information

Measuring Dipole Inversion in Self-Assembled Nano-Dielectric Molecular Layers

Li Zeng,[1,2] Riccardo Turrisi,[3] Bo Fu,[4] Jonathan D. Emery,[2,5] Amanda R. Walker,[6] Mark A. Ratner,[6] Mark C. Hersam,[1,2,5,6]Antonio F. Facchetti,*[,6] Tobin J. Marks,*[,1,2,5,6] Michael J. Bedzyk*[,1,2,4,5]

[1]Applied Physics Program, Northwestern University, 2220 Campus Drive. Evanston, Illinois 60208, USA

[2] Materials Research Science and Engineering Center, Northwestern University, Evanston, Illinois 60208, USA

[3] Materials Science Department, University of Milano-Bicocca, Via R. Cozzi 53, 20126 Milan, Italy

[4] Department of Physics and Astronomy, Northwestern University, 2145 Sheridan Road, Evanston, Illinois 60208, USA

[5] Department of Materials Science and Engineering, Northwestern University, 2220 Campus Drive. Evanston, Illinois 60208, USA

[6] Department of Chemistry, Northwestern University, 2145 North Sheridan Road, Evanston, Illinois 60208, USA

Corresponding Authors:

E-mail: bedzyk@northwestern.edu (M.J.B.)
E-mail: t-marks@northwestern.edu (T.J.M.)
E-mail: a-facchetti@northwestern.edu (A.F.F.)

Si/Mo multilayer preparation

Single crystal silicon wafers were cleaned by piranha solution (70% H_2SO_4 +30% H_2O_2) and then washed with a copious amount of deionized (DI) water and dried under N_2 flow. The subsequent 60 Si/Mo bilayers (period *d= 6.0 nm* with Si:*~4.5 nm* and Mo:*~1.5 nm*) with Si as the topmost terminating layer were deposited via magnetron sputtering deposition by the Advanced Photon Source (APS) Optics Group at Argonne National Laboratory (ANL). Prior to SAND/ISAND deposition, Si/Mo multilayer substrates were cleaned by repeated sonication of acetone and isopropyl alcohol and subjected to a 5 min oxygen plasma cleaning process.

Trilayer SAND/I-SAND sample preparation

The capping HfO_x and bottom prime ZrO_x were synthesized through sol-gel process, and PAE/IPAE monolayer were self-assembled on ZrO_x. 73 mM ethanol solution of $HfCl_4$ and 100 mM of $ZrCl_2$ were prepared with the mixture of nitric acid and DI water (molar ratio, metal chloride: HNO_3: H_2O=1:10:10) was then added under ambient conditions. The mixed precursor solutions were stirred overnight to reach full hydrolysis. Prior to film deposition, 7 mM HfO_x and 20 mM ZrO_x precursor solutions were prepared individually through dilution with ethanol. The first ZrO_x prime layers were synthesized by spin-coating the 20 mM $ZrCl_2$ ethanol solution on substrates for 30 sec with 5000 rpm, and annealing in ambient for 30 min at 150 °C for film oxides film formation and densification. Then the ZrO_x-primed substrates (Si and Si/Mo) were immersed in a preheated 3.0 mM phosphonic-acid based π-electron (PAE) and inverted PAE (IPAE) methanol solutions for 1 hr at 60 °C. After rinsing the coated substrates with methanol and blow-drying, the 7 mM HfO_x precursor solution was spin-coated (30 sec, 5000 rpm) on, followed by 30 min annealing at 150 °C to form the capping HfO_x layer. [1,2] The procedure of the SAND-based TFT shown in Figure 1 can be found in the previous reference.[1]

The extraction of X-ray fluorescence yields.

The Br Kα, Zr Kα, and Hf Lα XRF peaks at each incident angle were fitted with Gaussian functions on a linear background. The extracted peak areas at each angle were subsequently corrected for X-ray footprint, detector dead-time effects, fluorescence X-ray transmission factors, Vortex XRF detector efficiency and normalized to the incident X-ray intensity. Finally, the fluorescence yields of Br, Hf, and Zr were all normalized to unity at the high-angle limit of the scan range where the reflectivity approached zero.

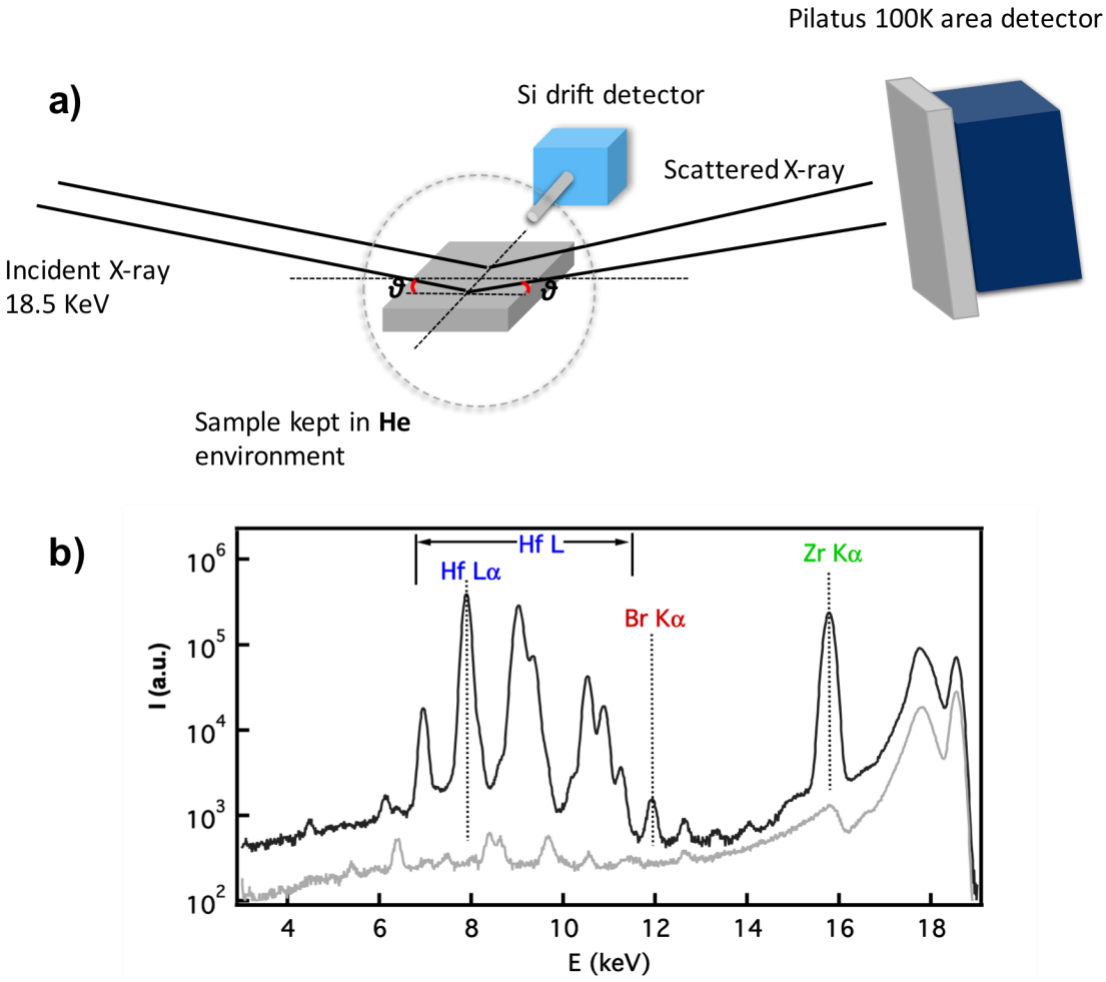

Figure S1. *(a) Schematic of LP-XSW measurement setup. (b) A representative XRF spectrum of SAND on Si/Mo multilayer collected at* $\theta = 0.25°$. *The Hf Lα fluorescence peaks (blue), Br Kα fluorescence (red) and Zr Kα fluorescence (green) are highlighted. The gray line is a XRF spectrum from a blank Si/Mo multilayer substrate at* $\theta = 0.25°$ *with the same experimental condition to ensure that the Hf, Br and Zr peaks were originating from the SAND film.*

XRR Data Analysis

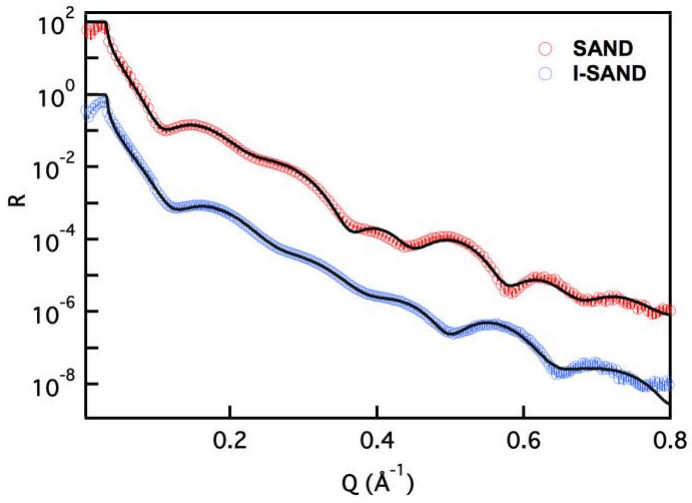

Figure S2. *X-ray reflectivity of trilayer SAND and I-SAND deposited on Si substrate. The black solid lines are the best-fit results. The SAND data and curve are vertically offset by ×100 for purposes of clarity.*

Table S1: The atomic and electron areal densities. The first three columns are the XRF measured elemental coverages. The fourth and fifth columns are the areal electron densities based on the XRF coverages. The sixth and seventh columns are areal electron densities based on XRR.

	Hf (nm^{-2})	Br (nm^{-2})	Zr (nm^{-2})	HfO_2[a] (e/Å^2)	ZrO_2[a] (e/Å^2)	HfO_2[b] (e/Å^2)	ZrO_2[b] (e/Å^2)
PAE	33.2	0.17	57.7	29.2	32.3	26.7	33.0
IPAE	30.9	0.18	54.7	27.2	30.6	26.2	30.4

a. Areal electron density calculated from XRF-derived elemental coverage. This assumes that the HfO_x and ZrO_x layers have the HfO_2 and ZrO_2 stoichiometry, respectively.
b. Areal electron densities are calculated from the XRR-derived maxima in the electron density profiles shown in Fig. 2. These maxima values are then multiplied by the XRR determined layer thicknesses.

DFT simulation details

Density functional theory (DFT) calculations using a plane-wave basis are employed to optimize the geometry of both PAE and IPAE. The exchange-correlation potential is treated by the PBE (Perdew-Burke-Ernzerhof) generalized gradient approximation. The atomic cores were described by the pseudopotentials generated by projector augmented wave (PAW) method. The electronic wave functions were represented on a plane wave basis set with a cutoff energy of 400 eV. The molecule is placed in a 30 Å × 30 Å × 30 Å periodic box. The size of the box was chosen large enough to eliminate the interaction between the molecule and its images. The optimized geometry of the molecule is then obtained by allowing the nuclei of all the free atoms to relax until the residual forces on all these ions are less than 0.025 eV/ Å. All DFT calculations were performed with the Vienna Ab *initio* Software Package (VASP). The optimized structures of PAE and IPAE are shown in Figure S3, and S4.

Mulliken charge analysis

The Mulliken charge reported from the DFT simulation results were listed below. The Figure S3 and Figure S4 were used to present number label of each atom for both PAE and IPAE case respectively. The net charges of moieties marked with grey dash lines in Figure 4c were calculated by summing up the charges inside.

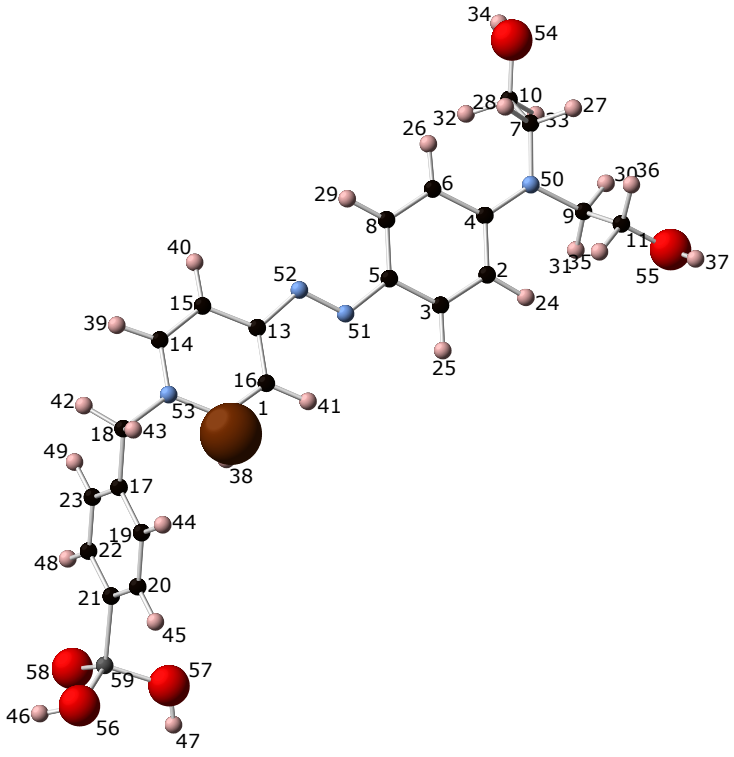

Figure S3. The optimized structure of PAE molecule with the numerical labels of atoms.

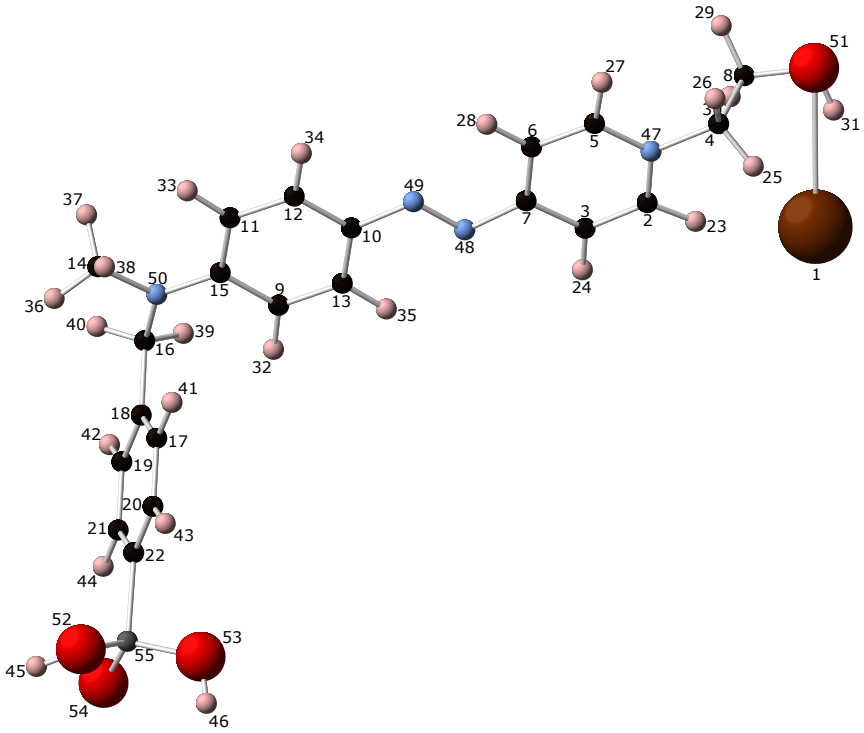

Figure S4. The optimized structure of IPAE molecule with the numerical labels of atoms.

Table S2. Mulliken charge population analysis of PAE molecule

label	atom	population
1	C	-0.35591
2	C	-0.341614
3	C	0.384105
4	C	0.210027
5	C	-0.337415
6	C	-0.420114
7	C	-0.327462
8	C	-0.420373
9	C	-0.220789
10	C	-0.221435
11	C	-0.120511

12	C	0.243035
13	C	-0.109254
14	C	-0.30483
15	C	-0.263805
16	C	0.186606
17	C	-0.481154
18	C	-0.333496
19	C	-0.238797
20	C	-0.054153
21	C	-0.35115
22	C	-0.289966
23	N	-0.222892
24	N	-0.125271
25	N	-0.190919
26	N	-0.020405
27	O	-0.541534
28	O	-0.542203
29	O	-0.668054
30	O	-0.658378
31	O	-0.60816
32	P	1.019657
33	H	0.254787
34	H	0.261783
35	H	0.251928
36	H	0.262206
37	H	0.251724
38	H	0.278047
39	H	0.260931
40	H	0.250978
41	H	0.193007
42	H	0.182292
43	H	0.424726
44	H	0.196516
45	H	0.182127
46	H	0.42553
47	H	0.345347
48	H	0.252436
49	H	0.270127
50	H	0.295802
51	H	0.240785
52	H	0.343347
53	H	0.335719

54	H	0.271417
55	H	0.464694
56	H	0.470334
57	H	0.296461
58	H	0.238079
59	Br	-0.774523

Table S3. Mulliken charge population analysis of IPAE molecule

label	atom	population
1	C	-0.121893
2	C	-0.290026
3	C	-0.39483
4	C	-0.129805
5	C	-0.279192
6	C	0.238495
7	C	-0.220499
8	C	-0.311012
9	C	0.21122
10	C	-0.365018
11	C	-0.326472
12	C	-0.32416
13	C	-0.584168
14	C	0.33892
15	C	-0.448891
16	C	-0.317516
17	C	0.200847
18	C	-0.303169
19	C	-0.242226
20	C	-0.343584
21	C	-0.057663
22	N	-0.042461
23	N	-0.181389
24	N	-0.133326
25	N	-0.218385
26	O	-0.549242
27	O	-0.669403
28	O	-0.660261
29	O	-0.605741
30	P	1.021048
31	H	0.328858

32	H	0.293485
33	H	0.307535
34	H	0.229358
35	H	0.268401
36	H	0.295263
37	H	0.191763
38	H	0.210837
39	H	0.437994
40	H	0.267771
41	H	0.25927
42	H	0.257859
43	H	0.286196
44	H	0.257778
45	H	0.22941
46	H	0.230207
47	H	0.261792
48	H	0.272454
49	H	0.27451
50	H	0.246109
51	H	0.265875
52	H	0.298938
53	H	0.465625
54	H	0.47261
55	Br	-0.800103

Table S4. DFT-calculated dipole moments of both PAE and IPAE molecules.

	Total dipole moment $\|\boldsymbol{p}\|$ (Debye)	Dipole moment along the surface normal direction (Debye)
PAE	12.4	3.04
IPAE	23.5	-0.70

The probability distribution of the degree of IPAE molecular tilting is quantified by the Boltzmann probability $\mathrm{P_B} = e^{\left[-\frac{\mathrm{E}(z_N+)-\mathrm{E}_{min}}{k_B T}\right]}$ for various molecular configuration. This is achieved by allowing the upper part of IPAE rotating around its C-N bond (marked as I_{23} axis in

Figure S5). The rotation of the upper part of IPAE by an angle γ will change the angle between axis I_{12} and I_{34}, and lead to change in the rotation angle α of IPAE. In total, 31 molecular states that associate with different Bromide vertical locations were calculated by rotating the upper IPAE around I_{23} axis by 31 angles sampled from -60˚ to 90˚ by every 5˚. The geometry of each molecule state was then relaxed with the four atoms 1,2,3,4 (see Figure S5) fixed. The energies and molecule heights of these relaxed molecular states were used to give the Boltzmann probability distribution $P_B = e^{\left[-\frac{E(z_{N+})-E_{min}}{k_B T}\right]}$ as a function of molecule height as shown in Figure 4d. Similar procedure was also used for

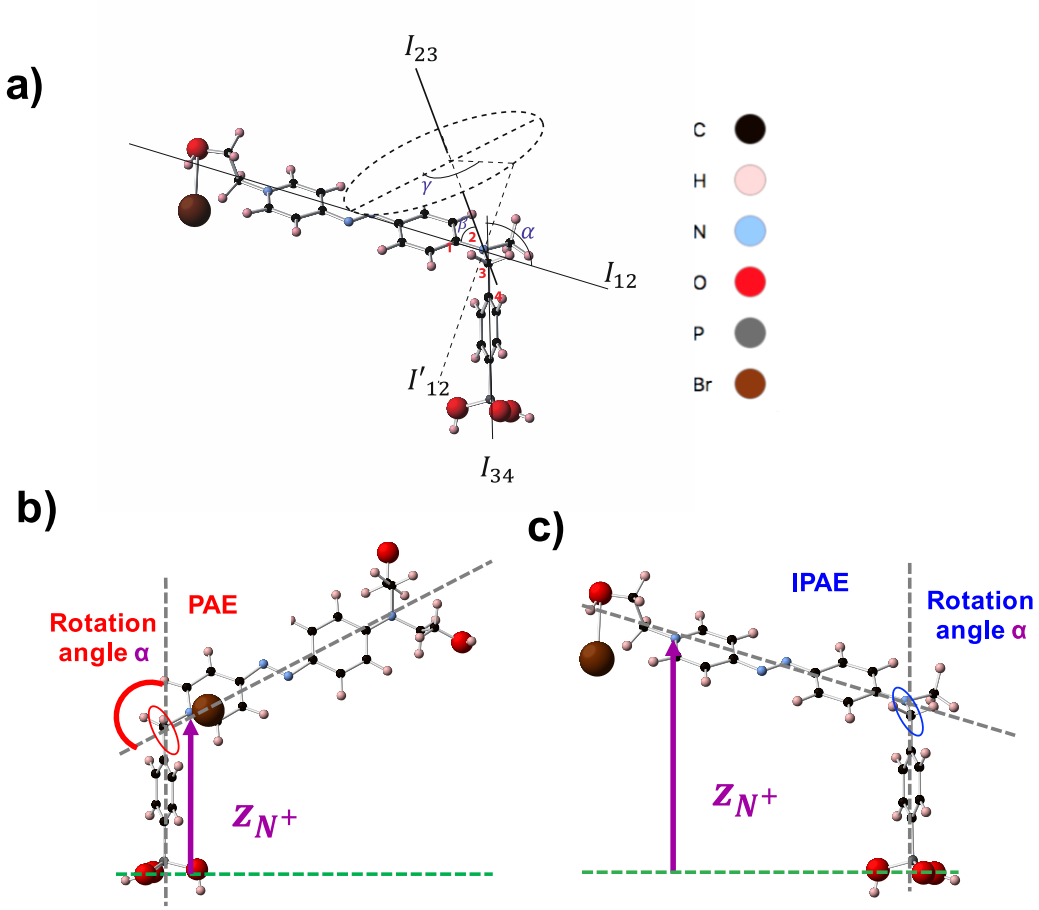

Figure S5. (a) A schematic illustration of the rotations implemented to obtain different molecular structure and tilting for IPAE molecule. Atom 1~4 were marked as they were manually placed to define the rotation angle α and fixed during the subsequent structure relaxation. I_{xy} was defined as the axis passing through atom x and y. The angle α between axis I_{34} and I_{12} was controlled by rotating I_{12} γ degree around axis I_{23}. (β is a fixed angle). (b) The rotation angle α was controlled by the carbon (atom #18 in Figure S2) sp^3 hybridization bond angle as indicated by the red circle. (c) The optimized structure of IPAE. The blue circle highlighted both nitrogen and carbon atoms (atom #50 and #16 in Figure S3), which introduced an additional freedom to rotate. In both cases, z_{N^+} is defined as the distance between the +1 quaternized nitrogen in the pyridine group and the bottom plane formed by the three oxygen atoms of PAE or IPAE molecule.

References:

(1) Ha, Y. G.; Emery, J. D.; Bedzyk, M. J.; Usta, H.; Facchetti, A.; Marks, T. J. Solution-Deposited Organic-Inorganic Hybrid Multilayer Gate Dielectrics. Design, Synthesis, Microstructures, and Electrical Properties with Thin-Film Transistors. *J. Am. Chem. Soc.* **2011**, *133*, 10239-10250.
(2) Everaerts, K.; Emery, J. D.; Jariwala, D.; Karmel, H. J.; Sangwan, V. K.; Prabhumirashi, P. L.; Geier, M. L.; McMorrow, J. J.; Bedzyk, M. J.; Facchetti, A.; Hersam, M. C.; Marks, T. J. Ambient-Processable High Capacitance Hafnia-Organic Self-Assembled Nanodielectrics. *J. Am. Chem. Soc.* **2013**, *135*, 8926-8939.